

Article

Characterization of Carboxylic Acid Reductase from *Mycobacterium phlei* Immobilized onto Seplite LX120

Rose Syuhada Basri ^{1,2}, Raja Noor Zaliha Raja Abd. Rahman ^{1,3}, Nor Hafizah Ahmad Kamarudin ^{1,4}, Wahhida Latip ¹ and Mohd Shukuri Mohamad Ali ^{1,2,*}

¹ Enzyme and Microbial Technology Research Center, Faculty of Biotechnology and Biomolecular Sciences, Universiti Putra Malaysia, Serdang 43400, Selangor, Malaysia

² Department of Biochemistry, Faculty of Biotechnology and Biomolecular Sciences, Universiti Putra Malaysia, Serdang 43400, Selangor, Malaysia

³ Department of Microbiology, Faculty of Biotechnology and Biomolecular Sciences, Universiti Putra Malaysia, Serdang 43400, Selangor, Malaysia

⁴ Centre of Foundation Studies for Agricultural Science, Universiti Putra Malaysia, Serdang 43400, Selangor, Malaysia

* Correspondence: mshukuri@upm.edu.my

Abstract: A multi-domain oxidoreductase, carboxylic acid reductase (CAR), can catalyze the one-step reduction of carboxylic acid to aldehyde. This study aimed to immobilize bacterial CAR from a moderate thermophile *Mycobacterium phlei* (*MpCAR*). It was the first work reported on immobilizing bacterial CAR onto a polymeric support, Seplite LX120, via simple adsorption. Immobilization time and protein load were optimized for *MpCAR* immobilization. The immobilized *MpCAR* showed optimal activity at 60 °C and pH 9. It was stable over a wide range of temperatures (10 to 100 °C) and pHs (4–11), retaining more than 50% of its activity. The immobilized *MpCAR* also showed stability in polar solvents. The adsorption of *MpCAR* onto the support was confirmed by Scanning Electron Microscopy (SEM), Fourier-Transform Infrared (FTIR) spectroscopy, and Brunauer–Emmett–Teller (BET) analysis. The immobilized *MpCAR* could be stored for up to 6 weeks at 4 °C and 3 weeks at 25 °C. Immobilized *MpCAR* showed great operational stability, as 59.68% of its activity was preserved after 10 assay cycles. The immobilized *MpCAR* could also convert approximately 2.6 mM of benzoic acid to benzaldehyde at 60 °C. The successfully immobilized *MpCAR* on Seplite LX120 exhibited improved properties that benefit green industrial processes.

Keywords: carboxylic acid reductase; *Mycobacterium phlei*; characterization; immobilization; stability



Citation: Basri, R.S.; Rahman, R.N.Z.R.A.; Kamarudin, N.H.A.; Latip, W.; Ali, M.S.M. Characterization of Carboxylic Acid Reductase from *Mycobacterium phlei* Immobilized onto Seplite LX120. *Polymers* **2022**, *14*, 4375. <https://doi.org/10.3390/polym14204375>

Academic Editor: Marina G. Holyavka

Received: 27 August 2022

Accepted: 3 October 2022

Published: 17 October 2022

Publisher's Note: MDPI stays neutral with regard to jurisdictional claims in published maps and institutional affiliations.



Copyright: © 2022 by the authors. Licensee MDPI, Basel, Switzerland. This article is an open access article distributed under the terms and conditions of the Creative Commons Attribution (CC BY) license (<https://creativecommons.org/licenses/by/4.0/>).

1. Introduction

Over the decades, many efforts have been devoted to researching potentially robust aldehyde-producing enzymes. Aldehydes are organic compounds in the fine chemicals, pharmaceuticals, and flavor and fragrance industries. They are essential intermediates for preparing high-value-added compounds, such as alkanes, alcohols, and amines. Carboxylic acids are desirable precursors for aldehyde production as they are abundant, stable, and usually biologically synthesized [1–4]. Carboxylic acid reductase (CAR) is a large (~130 kDa) multi-domain enzyme that can catalyze the one-step reduction of carboxylic acids to corresponding aldehydes with the availability of cofactors; adenosine triphosphate (ATP) and nicotinamide adenine dinucleotide phosphate (NADPH), and this enzyme demands post-translational modification for its activation [5].

CAR (EC 1.2.1.30) belongs to the aldehyde oxidoreductase group, where its first gene, *car*, was cloned, expressed, and characterized from *Nocardia* sp. [6]. The structure of CAR is relatively complex. It consists of an N-terminal adenylation domain (A domain), a thiolation domain (T domain), and a C-terminal reductase domain (R domain). Generally, the irreversible reduction of carboxylic acids to aldehydes involves three key steps: (i) Adenylation: ATP-dependent activation of the acid by the A domain, which results in the

formation of an acyl adenylate intermediate; (ii) Thiolation: transfer of the acyl intermediate to the phosphopantetheine linker; and (iii) Reduction: the NADPH-dependent reduction of the acyl-thioester produces the corresponding aldehyde product [5]. For the enzyme to be in the holo form (active), a phosphopantetheine group (also known as ‘swinging arm’) needs to be attached to the conserved serine in the T domain. A phosphopantetheine transferase enzyme (PPTase) is required for CAR activity to be maximal. PPTase helps in the covalent attachment of the phosphopantetheine group [7]. The most co-expressed PPTase was the surfactin phosphopantetheinyl transferase (Sfp) from *Bacillus subtilis* [8–13].

Enzyme usage for industrial applications and commercialization purposes is broadly recognized, yet their stability and cost are treated as a limitation. The structural stability of some enzymes is highly challenged during biochemical reactions. In addition to eliminating those obstacles, enzyme immobilization is a promising approach for obtaining superior biocatalysts. Immobilized enzymes are physically confined or localized in a defined space region with retention of their catalytic activities, which can be used repeatedly and continuously [14]. A few established immobilization methods include physical adsorption, cross-linking, covalent bonding, encapsulation, and entrapment [15,16]. Each method has its advantages and disadvantages and may contribute to significant variations in the properties of the immobilized enzymes. In general, enzyme immobilization is limited by low binding on the support, lack of biocompatibility, and commonly lower residual activity than free enzyme. Some recent immobilization methods, such as metal-protein hybrids and enzyme immobilization using biocompatible supports, retain higher residual activity [17,18]. Among all the methods, physical adsorption is the simplest technique for enzyme immobilization. It depends on the enzyme-support’s van der Waals forces, hydrogen bonds, and ionic bonding. Via this method, no chemical bonding is involved between the support and enzymes, and therefore no or less significant changes to the enzyme structure [19]. Enzymes immobilized via the adsorption method have demonstrated improved properties such as retaining higher catalytic efficiency and residual activity, thermal and pH tolerance, storage stability, and recyclability [20–23].

Another important prerequisite in enzyme immobilization is the selection of suitable carriers or supports. Immobilization on ionic exchange resins is generally known to be simpler than on other supports. There are ionic and electrostatic interactions involved between the protein and the oppositely charged resin. Cationic exchangers have cations as their active ions, while anionic exchangers have anions. The enzyme is only attached to the support when there are high enough ionic bridges formed between the protein and the support to counterbalance the ionic strength of the surrounding medium [24]. This strategy minimizes the enzyme chemical modification to only the protein groups involved during the immobilization process [25]. CAR’s catalytic activity involves all three domains and occurs sequentially from A- to T- and later to R-domain, which requires high flexibility and mobility. Therefore, immobilization using ionic resins is considered suitable for CAR since the attachment of the enzyme onto the support is only at a certain region. This method will not totally ‘immobilize’ the whole CAR protein structure. Other advantages of utilizing the ionic exchange resin concept include support recovery, non-expensive, and high availability of resins. Commonly, ion exchange resins are made of polymers. Many polymeric resins have been used for many enzymes. Polymers can protect biomolecules from denaturation, inactivation, and structural damage while maintaining high catalytic activity [15].

Carboxylic acid reductase from *Mycobacterium phlei* (*MpCAR*) was initially expressed and characterized by Finnigan et al. [26]. The enzyme is among the most thermostable CARs known to date, as it can retain 92% of its catalytic activity at 42 °C and has a residual activity of up to 50 °C. Moreover, *MpCAR* showed the longest half-life, 123.2 h at 30 °C [26]. This enzyme showed a great pH tolerance of >50% activity between pH 4.3 and 11.8 [27]. Due to the thermostability of the enzyme, *MpCAR* has been involved in an in vitro enzyme cascade reaction developed using a mathematical model with other enzymes, including esterase and aldehyde dehydrogenase, for the generation of 4-methylbenzyl alcohol [28]. Additionally, it is still early in the day for the immobilization of CARs. CAR immobilization was first

tried using EziG Opal, a commercial support with 26% enzyme weight on the carrier and more than 59% activity recovery [29]. Recently, a CAR from *Pycnoporus cinnabarinus* fungus was immobilized onto nickel sepharose resin and achieved 82% and 76% of immobilization yield and efficiency, respectively [30].

In an attempt to create diversity in the toolbox of available CARs that may contribute to the development of sustainable and green chemistry routes, in this research, a carboxylic acid reductase from a moderate thermophile, *Mycobacterium phlei* (MpCAR), was immobilized onto the commercial support Sephrite LX120 via an adsorption method. This new polymeric support is an ionic resin that is supposed to provide gentle binding for the enzyme and allow the structure to maintain its flexibility, besides taking advantage of the simplicity of the immobilization process. The immobilization conditions were optimized by considering the immobilization time and protein load. The successful immobilization of MpCAR was confirmed by enzyme activity assay, Brunauer–Emmett–Teller (BET) analysis, and Fourier-Transform Infrared (FTIR) spectroscopy analysis. In addition, the properties of the immobilized enzyme at different temperatures and pHs were also explored. The morphology of the support before and after CAR binding was characterized by using Scanning Electron Microscopy (SEM). More importantly, the storage stability, reusability, bioconversion ability, and the effect of organic solvents on immobilized MpCAR were all investigated to determine the potential industrial applicability of this enzyme.

2. Materials and Methods

2.1. Chemicals, Reagents, and Equipment

All chemicals and equipment used in this study were obtained from the Enzyme and Microbial Technology (EMTech) Research Center, Faculty of Biotechnology and Biomolecular Sciences, Universiti Putra Malaysia.

2.2. Preparation of Purified Recombinant MpCAR

The gene sequence of MpCAR was extracted from the NCBI database (WP_003889896.1) and was codon optimized for expression in *Escherichia coli*. The gene was synthesized by Integrated DNA Technologies (IDT). The MpCAR gene was cloned into pET51b and transformed into *E. coli* BL21 (DE3). MpCAR was co-transformed with a pET28a vector containing a phosphopantetheine transferase from *Anoxybacillus geothermalis* strain D9. Cells were cultured at 25 °C and expressed using 0.75 mM of isopropyl β -d-1-thiogalactopyranoside (IPTG) in Luria Bertani media for 20 h. The cells were harvested through centrifugation at 10,000 rpm for 30 min at 4 °C. The cells were then resuspended with a buffer (20 mM HEPES pH 7.4 containing 20 mM of imidazole and 500 mM of NaCl), lysed by sonication, and centrifuged again at 10,000 rpm for 30 min to collect the soluble proteins. A one-step purification was done by using nickel affinity chromatography. The column was equilibrated with a binding buffer (20 mM HEPES pH 7.4 containing 20 mM of imidazole and 500 mM of NaCl) and then loaded with the crude enzyme. The column was washed with a washing buffer for up to 5 column volumes. The purified protein underwent gradient elution using an elution buffer (20 mM HEPES pH 7.4 containing 500 mM of imidazole and 500 mM of NaCl). The eluted purified protein from each fraction was then measured for protein content using the Bradford assay and the enzyme activity assay at 340 nm (as mentioned in Sections 2.3 and 2.4, respectively). The purified enzymes were stored at 4 °C.

2.3. Protein Content Determination

The Bradford assay was used to determine the protein concentration [31]. It was conducted using the commercial Bradford reagent from Sigma. The absorbance was measured at 595 nm. Bovine serum albumin (BSA) was used as the protein standard.

2.4. Enzyme Activity Assay of MpCAR

The assay was modified from the previously published method [32]. It was conducted in 100 mM of HEPES pH 7.5, 1 mM of ATP, 0.25 mM of NADPH, 10 mM of MgCl₂, 10 μ L

(0.5 mg/mL) of purified *MpCAR* solution, or 10 mg of immobilized *MpCAR* (7.5 mg *MpCAR*/g of Seplite LX120 (after optimization)), and 5 mM of benzoic acid as substrate, in a total reaction volume of 200 μ L. The assay was performed in triplicate at the optimum temperature (40 $^{\circ}$ C for the free enzyme and 60 $^{\circ}$ C for the immobilized enzyme) for 10 min of incubation. The assay for free *MpCAR* was conducted in a 96-well microplate. In contrast, for immobilized *MpCAR*, the 10 min assay incubation was conducted in a round-bottom 2 mL microcentrifuge tube before the supernatant was transferred to the 96-well microplate for an absorbance reading. The NADPH oxidation was measured at 340 nm. Control reactions were performed by incubating all the assay components without the presence of the enzyme. One unit of CAR activity was defined as the rate of 1 μ mole of NADPH consumed per minute. The enzyme activity and relative activity were calculated as below:

$$\text{Free enzyme activity (U/mL)} = \frac{(\text{Absorbance of control} - \text{Absorbance of sample}) \div \text{Gradient of NADPH curve}}{\text{Incubation time} \times \text{Volume of free enzyme}}$$

$$\text{Immobilized enzyme activity (U/g)} = \frac{(\text{Absorbance of control} - \text{Absorbance of sample}) \div \text{Gradient of NADPH curve}}{\text{Incubation time} \times \text{Weight of immobilized enzyme}}$$

$$\text{Relative activity (\%)} = \frac{\text{Enzyme activity}}{\text{Initial enzyme activity}} \times 100$$

2.5. Immobilization of Purified *MpCAR*

The immobilization optimization was performed to determine the optimal conditions for the immobilization of *MpCAR*. The optimization included the immobilization time and the protein load. The immobilized enzyme activity and the immobilization yield were recorded.

2.5.1. Effect of Immobilization Time of *MpCAR*

The effect of time on the immobilization of *MpCAR* was conducted by mixing enzyme solution with Seplite LX120 (5 mg of protein/g of Seplite LX120) in 20 mM of HEPES pH 7.5 buffer and stirring over different periods (30, 60, 90, 120, and 150 min) at 25 $^{\circ}$ C in separate beakers. The mixture was stirred at 250 rpm. The mixture was then filtered and dried at 30 $^{\circ}$ C for 90 min in a fluid bed dryer. The unbound enzyme was measured for protein content. The immobilized *MpCAR* was assayed for its enzyme activity. The immobilization yield was calculated as below:

$$\text{Immobilization yield (\%)} = \frac{(\text{Initial protein content} - \text{Unbound protein content})}{\text{Initial protein content}} \times 100$$

2.5.2. Effect of Immobilization Protein Load of *MpCAR*

The determination of the optimal enzyme concentration to be loaded onto the support was completed by varying the enzyme concentrations (2.5, 5.0, 7.5, 10.0, 12.5, and 15.0 mg of *MpCAR*/g of Seplite LX120). Each mixture was incubated for 90 min (based on the optimum adsorption time determined earlier) at 25 $^{\circ}$ C and stirred at 250 rpm. The mixture was then filtered and dried at 30 $^{\circ}$ C for 90 min. The unbound enzyme was measured for protein content. The immobilized *MpCAR* was assayed for its enzyme activity. The immobilization yield was also calculated using the equation shown in Section 2.5.1.

2.6. Characterization of the Immobilized and Free *MpCAR*

2.6.1. Effect of Temperature

The effect of temperature on the catalytic activity of immobilized *MpCAR* was measured at temperatures ranging from 20 to 80 $^{\circ}$ C, at 10 $^{\circ}$ C intervals, for 10 min. It was then assayed spectrophotometrically. The temperature stability of the immobilized *MpCAR* was tested by preincubating the immobilized *MpCAR* at different temperatures (10 to 100 $^{\circ}$ C,

with 10 °C intervals) for 30 min before being assayed at 60 °C for 10 min. The control used for this experiment was the untreated enzyme.

2.6.2. Effect of pH

The effect of pH on immobilized *MpCAR* activity was evaluated at pH 4–11, by using 50 mM sodium acetate (pH 4–6), 50 mM sodium phosphate (pH 6–8), 50 mM Tris HCl (pH 8–9), and 50 mM glycine NaOH (pH 9–11). The activity assay using these different buffers was performed at 60 °C for 10 min. Moreover, the pH stability of the immobilized *MpCAR* was determined by preincubating the 10 mg immobilized *MpCAR* at different pH values ranging from pH 4–11 at 50 °C for 30 min. The mixture was then subjected to the activity assay at 60 °C for 10 min.

2.6.3. Effect of Organic Solvents

A stability study of the immobilized *MpCAR* towards different organic solvents was conducted. Ten mg of immobilized *MpCAR* were mixed with 100 mM HEPES buffer pH 7.5 and 25% (*v/v*) organic solvents before preincubating for 30 min at 50 °C. The preincubated immobilized enzyme was then assayed at 60 °C for 10 min for enzyme activity. A control reaction (all assay components including the respective solvent but without the presence of enzyme) was prepared for each set of enzyme and organic solvent. The same procedure was applied to the free enzyme, except the preincubation was done at 30 °C for 30 min and the assay was performed at 40 °C for 10 min. The untreated enzyme was assigned a value of 100% activity.

2.6.4. Scanning Electron Microscopy (SEM) and Brunauer–Emmett–Teller (BET) Analysis

The morphology, or surface features, of immobilized *MpCAR* were viewed via SEM. The sample was coated with gold before being analyzed under SEM. The images of the empty support and the immobilized *MpCAR* were captured under 20×, 500×, 5000×, and 10,000× magnifications. The surface area and pore characteristics of the immobilized *MpCAR* were determined by BET analysis with the nitrogen gas adsorption-desorption method using the MicroActive TriStar II Plus 2.03 surface area analyzer.

2.6.5. Fourier-Transform Infrared (FTIR) Spectroscopy

Structural analysis was conducted using FTIR spectroscopy. The measurement range was carried out at a spectrum range of 4000–500 cm⁻¹ and over 3 accumulation scans. The spectrometer radiation (IR) was from an attenuated total reflectance (ATR) crystal. A pressure controller was adjusted for optimal contact between the sample and the diamond plate before the measurements were recorded.

2.6.6. Storage Stability and Reusability Study

The storage stability of immobilized and free *MpCAR* was determined by measuring the enzyme activity after weeks of storage. The dry powder of immobilized *MpCAR* (7.5 mg *MpCAR*/g of Seplite LX120) and the free purified *MpCAR* (5 mg of *MpCAR* in 20 mM of HEPES pH 7.5) were stored at 4 and 25 °C, respectively. For the reusability test, 10 mg of immobilized *MpCAR* was weighed, placed in a 2 mL microcentrifuge tube, and prepared for the enzyme activity assay at pH 7.5. After each assay cycle, the mixture of immobilized *MpCAR* and other assay components was centrifuged to separate the supernatant from the immobilized enzyme (the pellet). The supernatant was then measured spectrophotometrically at 340 nm. The immobilized enzyme (pellet) was washed with buffer and allowed to air dry. This process was repeated ten times. The initial activity of the immobilized enzyme was calculated as being 100%.

2.7. Bioconversion Analysis of Immobilized MpCAR Using High-Performance Liquid Chromatography (HPLC)

The enzyme (10 mg of immobilized MpCAR (7.5 mg MpCAR/g of Seplite LX120)) was incubated with other assay components, as mentioned in Section 2.4. In separate microcentrifuge tubes, the reaction mixture was shaken moderately and incubated for 1 h at different incubation temperatures ranging from 20 to 60 °C (with 10 °C intervals). The supernatant was transferred to HPLC vials for analysis. Two individual experiments were performed, and the conversions of benzoic acid to benzaldehyde were quantified using HPLC-UV. HPLC-UV measurements were conducted, as explained in [33]. Benzaldehyde was detected at 254 nm. Product quantification was calculated using linear interpolation from the benzoic acid calibration curve. The bioconversion yield was calculated as below:

$$\text{Bioconversion yield (\%)} = \frac{\text{Concentration of product}}{\text{Concentration of substrate}} \times 100$$

3. Results and Discussion

3.1. Immobilization of MpCAR

Seplite LX120 is a highly cross-linked styrene-divinylbenzene copolymer (containing an amine functional group) used as the immobilization support for MpCAR. The immobilization of MpCAR onto Seplite LX120 was optimized by varying the immobilization time to determine the optimum time with the highest protein yield and immobilized enzyme activity. Five mg of protein/g of Seplite LX120 was used as the standard concentration for this parameter. Figure 1A represents a chart with immobilization yield (%) versus the immobilized enzyme activity (U/g) at different immobilization times, with 30 min intervals. Overall, the immobilization yield of the MpCAR gradually increased over time. MpCAR reached its 100% adsorption yield onto 1 g of Seplite LX120 support at 90 min of immobilization time. The activity of the immobilized enzyme was also found to be the highest (141.14 U/g) at 90 min into the immobilization process. Interestingly, the 100% immobilization yield was constant even at a longer period of immobilization, up to 180 min. Perhaps the enzyme-support affinity was good; hence, the enzymes remained attached to the support. However, even though the yield was high, the activity of immobilized enzymes was observed to drop after 90 min of immobilization. It was probably due to the excessive enzyme-support interaction time that offered multi-point binding and unnecessary structural rigidity, leading to enzyme inactivation [34]. Therefore, the optimal immobilization time for MpCAR onto Seplite LX120 was 90 min at 25 °C (room temperature).

Figure 1B depicts the effect of different protein concentrations loaded for the MpCAR immobilization onto 1 g of Seplite LX120 for 90 min of immobilization time (based on the previously optimized parameter). At the concentration of 2.5–7.5 mg of enzyme, approximately 99–100% of the immobilization yield was obtained. However, when the protein load was further increased to 10, 12.5, and 15 mg, the yield dropped to 95, 91, and 82%, respectively. Consequently, when 15 mg of protein was used, the activity of the immobilized enzyme decreased significantly to 112.06 U/g. Similar behavior was observed when optimizing the immobilization condition of puerarin glycosidase from *Microbacterium oxydans* CGMCC 1788 onto DEAE-52 cellulose [35]. The increase in protein load permits a greater available enzyme amount to interact with the support, increasing the support surface coating. However, a higher MpCAR load also causes the immobilization yield to decrease. The support may possibly have been fully coated by the MpCAR and reached its saturation limit when the amount of enzyme was ≥ 10 mg; hence the protein is prone to leach out from the support, causing yield reduction. Considering both immobilization yield and activity of the enzyme, the optimal concentration for protein loading was 7.5 mg MpCAR/g of Seplite LX120. Under these conditions, 99% yield and 184.4 U/g of immobilized MpCAR activity were achieved.

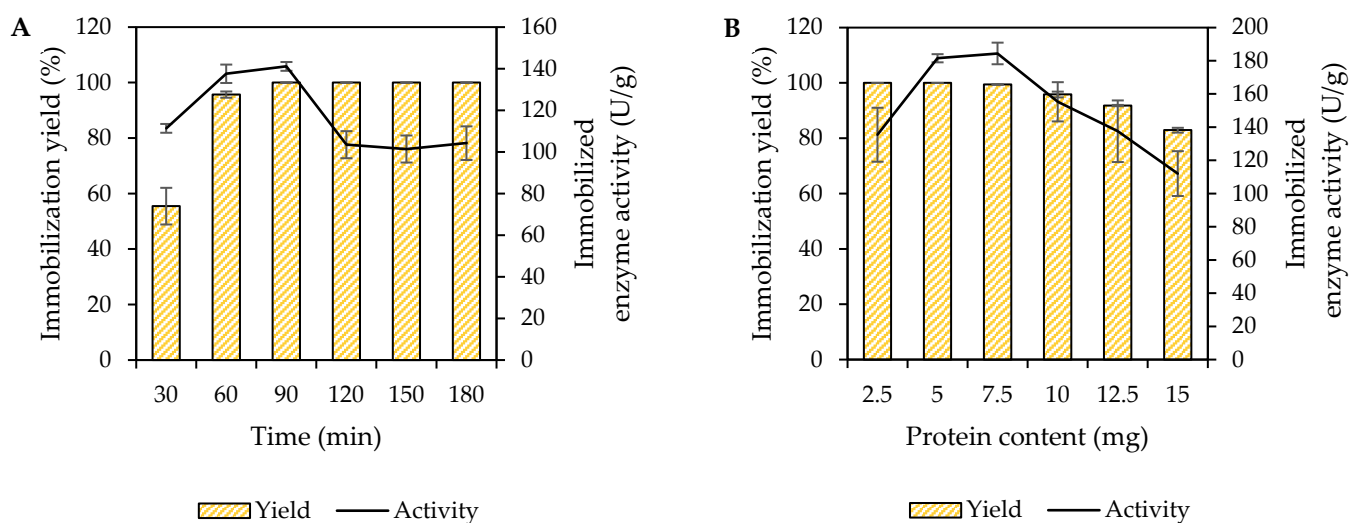


Figure 1. Immobilization optimization of carboxylic acid reductase from *Mycobacterium phlei* (*MpCAR*). **(A)** Effect of immobilization time on immobilization yield (%) and immobilized enzyme activity (U/g). The purified *MpCAR* (5 mg) was immobilized onto 1 g of Seplite LX120 at different immobilization times at 30 min intervals. **(B)** Effect of protein load on immobilization yield (%) and immobilized enzyme activity (U/g). Different protein contents (with 2.5 mg intervals) were loaded for their 90 min of immobilization onto Seplite LX120. The immobilization was performed at room temperature with a stirring speed of 250 rpm. Samples were measured in triplicates.

Ultimately, based on the optimization study, the best immobilization conditions were 1 g of Seplite LX120 as the support for 90 min immobilization of 7.5 mg of purified *MpCAR*. The stirring was maintained at 250 rpm, and the immobilization of *MpCAR* was conducted at 25 °C (room temperature). The schematic illustration of *MpCAR* immobilization and binding of the enzyme onto the support is presented in Figure 2.

3.2. Effect of Temperature on Activity and Stability of Immobilized *MpCAR*

The temperature dependence of the enzyme activity of immobilized *MpCAR* was studied at 10–90 °C. As shown in Figure 3A, the highest immobilized enzyme activity, equivalent to the optimal reaction temperature for immobilized *MpCAR*, was at 60 °C. The enzyme activity of the immobilized *MpCAR* rapidly decreased above 60 °C. A previous study showed free *MpCAR* to possess optimal activity at 42 °C [26]. The immobilized *MpCAR* exhibited an 18 °C increase in temperature optima compared to the free *MpCAR*. These data suggest that immobilization increased the resilience of the enzyme, making the immobilized *MpCAR* have better thermal tolerance than the free form. These results could be attributed to the interaction of the enzyme and support, which might impair conformational flexibility, requiring a higher temperature for the enzyme molecule to attain a proper conformation to maintain its reactivity. Hence, a sharp loss in activity above 60 °C might be due to the denaturation of enzyme molecules [36]. A similar result was obtained when an oxidoreductase laccase was immobilized and showed a higher optimal temperature (65 °C) than in its free form (55 °C). The interaction between the laccase and its immobilization support increased the activation energy to recognize the optimal conformation for substrate binding [37].

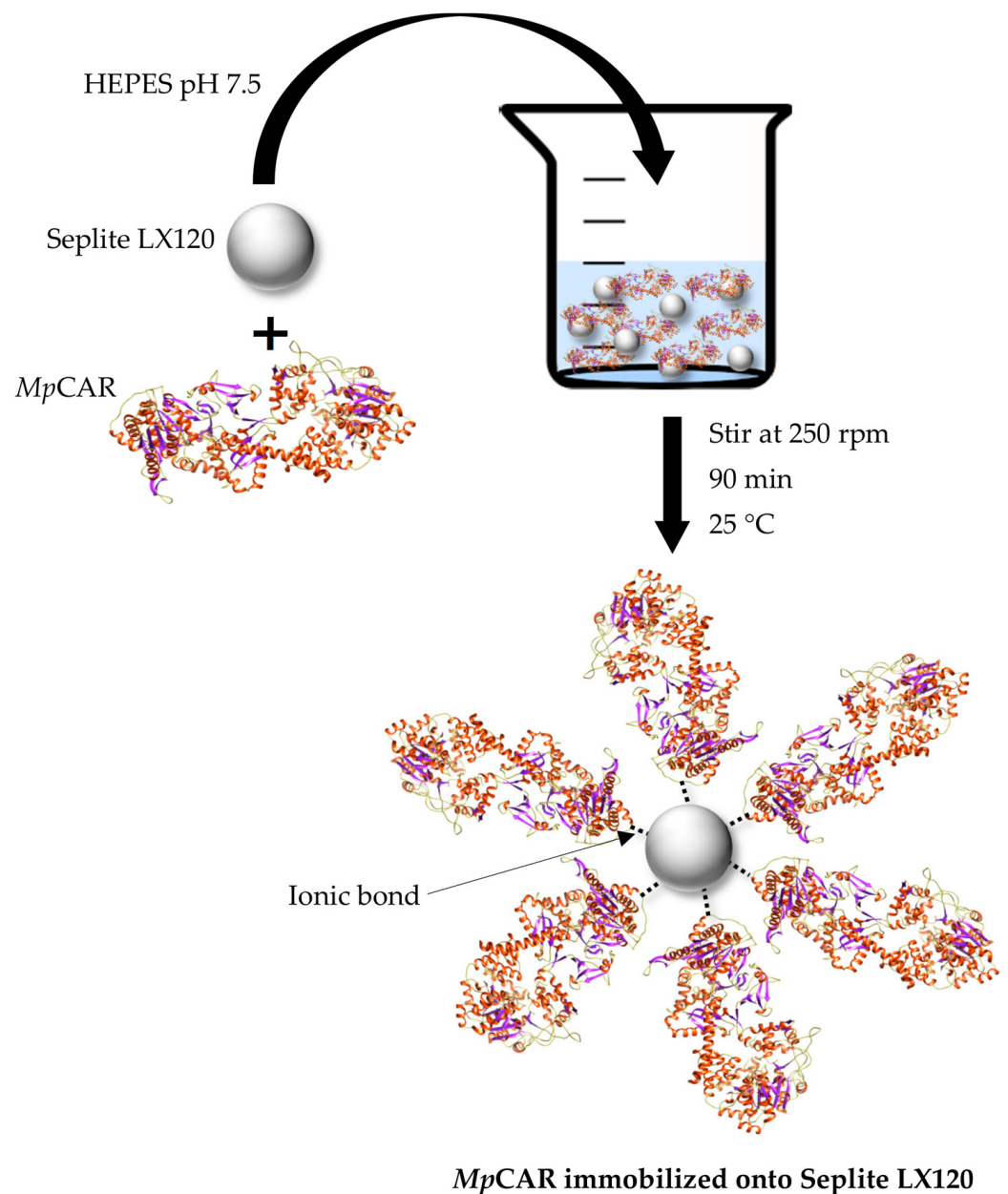


Figure 2. Schematic diagram illustrating the immobilization of carboxylic acid reductase from *Mycobacterium phlei* (*MpCAR*) onto Seplite LX120 via the adsorption method.

The thermal stability of immobilized *MpCAR* was determined by measuring the relative activity as a function of temperature in the range from 10 to 100 °C (Figure 3B). It was previously discovered that free *MpCAR* could retain its residual activity at temperatures as high as 50 °C [26]. In this study, the immobilized enzyme retained more than 60% of its relative activity across all temperatures tested, and the immobilized enzyme was found to be most stable at 50 °C. The immobilization method may have improved the conformational stability of the *MpCAR* enzyme in its native form. The Seplite LX120 may protect the enzyme by decreasing enzyme mobility and thermal vibrations, preventing unfolding and enzyme aggregation. It is usually found that an immobilized enzyme has higher thermal stability than a free enzyme due to the restriction of the enzyme's conformational flexibility. The enzyme became less flexible, possibly due to the attachment of the enzyme onto the support, which limits the conformational alterations and movements under different temperatures [38]. Therefore, the described immobilization process produced immobilized *MpCAR* with excellent thermal stability.

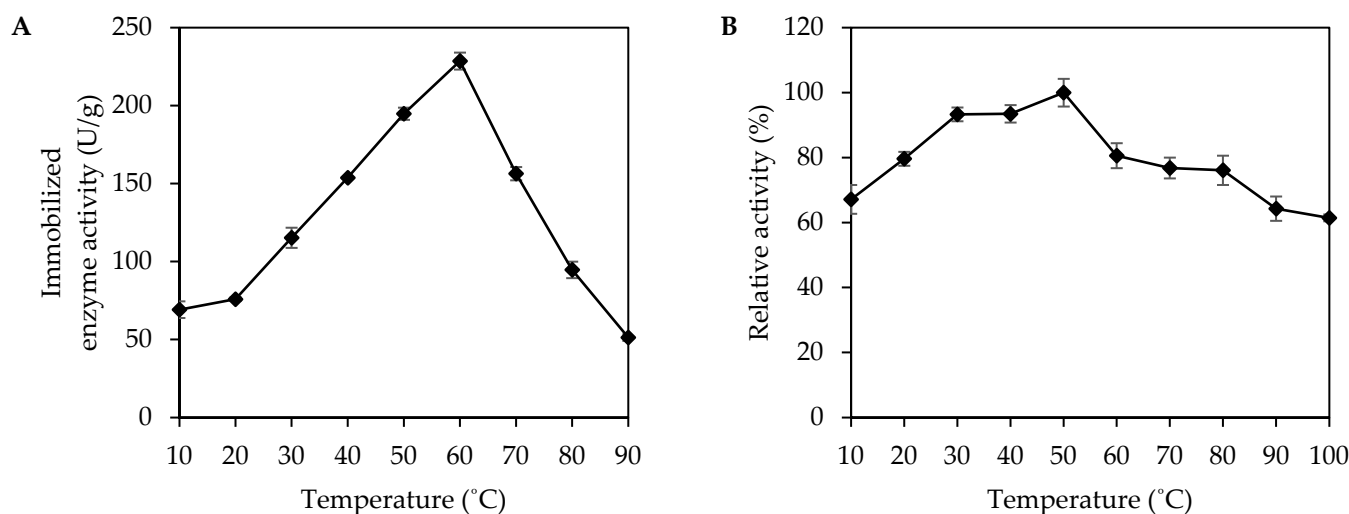


Figure 3. Characterization of immobilized carboxylic acid reductase from *Mycobacterium phlei* (*MpCAR*). The effect of temperature on the activity (A) and stability (B) of the immobilized *MpCAR*. The optimal temperature and thermal stability of immobilized *MpCAR* were measured at different temperatures ranging from 10 to 90 °C and from 10 to 100 °C, respectively. Samples were measured in triplicates.

3.3. Effect of pH on Activity and Stability of Immobilized *MpCAR*

The effect of pH on the immobilized enzyme activity depends on the enzyme, immobilization method, and support used. The effect of pH (4–11) on the activity of the immobilized *MpCAR* was studied. As shown in Figure 4A, the optimal pH corresponding to the highest activity of immobilized *MpCAR* was obtained at pH 9. In comparison, the free *MpCAR* showed optimal activity at pH 7.5 and decreased quickly as the pH increased [26]. The immobilization did cause a shift in the optimal pH for the activity of immobilized *MpCAR*, and the enzyme activity was also higher at high pH values, suggesting that the immobilized enzyme had improved alkaline resistance. The pH shifts upon immobilization probably occur due to secondary interactions between the enzyme and the polymeric support [36,39]. It may also be suggested that the Seplite LX120 is an anionic support as the enzyme immobilization causes a shift to the basic pH values [40]. The shift in optimal pH of the immobilized enzyme through simple adsorption has also been observed when pectinase was immobilized onto a cationic polystyrene resin [41].

The pH of the reaction highly influences the catalytic stability of enzymes. The influence of pH on the stability of immobilized *MpCAR* is shown in Figure 4B. The *MpCAR* immobilized onto Seplite LX120 remained stable (with ~50% retention in activity) within the entire pH range tested, from pH 4 to 11. In the pH range from 4 to 8, more than 80% of the relative enzymatic activity was retained, with 100% of *MpCAR* activity achieved at pH 7. While from pH 9–11, at least >50% of enzymatic activity was obtained, with the lowest value observed being 54% at pH 11. The free *MpCAR* was also found to have great pH tolerance, ranging from pH 4.3 to 11.8 [27]. This result showed that the immobilization procedure could maintain the stability of *MpCAR* over a broad pH range under extreme acidic and alkaline pHs. It was confirmed that the surrounding pH was responsible for the enzyme activity as it affected the ionization within the enzyme. Most probably, the immobilized *MpCAR* showed a strong affinity towards the substrate due to the orientation and readily available active sites of the enzyme [42,43].

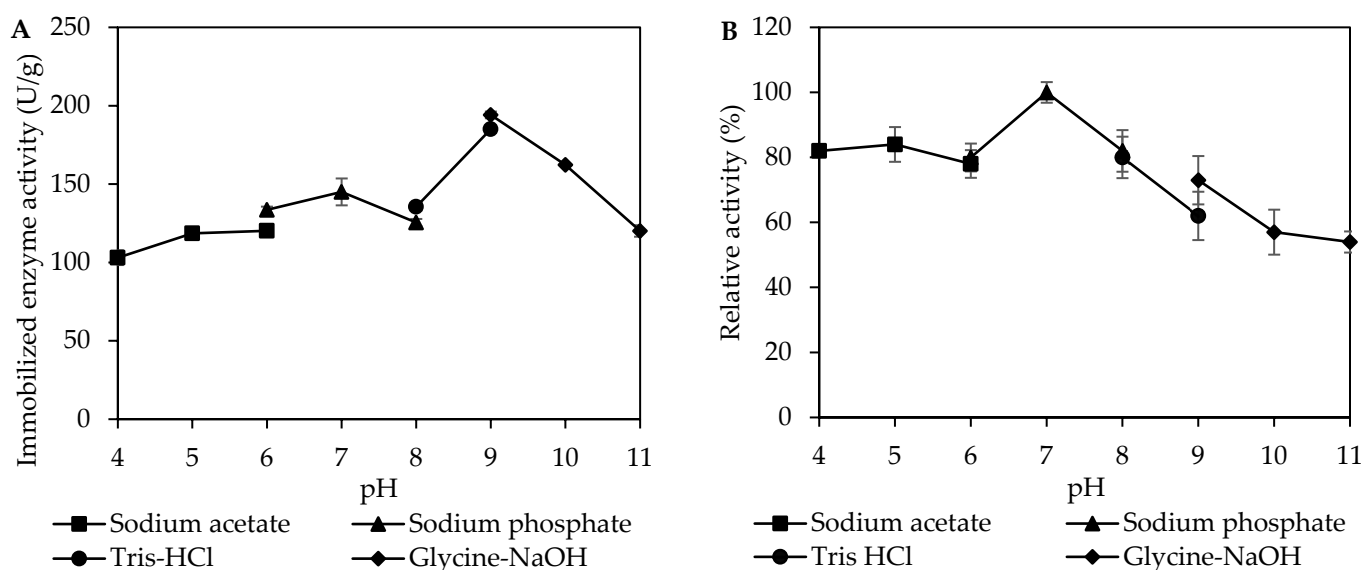


Figure 4. Characterization of immobilized carboxylic acid reductase from *Mycobacterium phlei* (*MpCAR*). The effect of pH on the activity (A) and stability (B) of the immobilized *MpCAR*. The optimal pH and pH stability of immobilized *MpCAR* were measured at different pH ranges from pH 4 to 11. Samples were measured in triplicates.

3.4. Effect of Organic Solvents on the Stability of Immobilized *MpCAR*

The effect of 25% (*v/v*) organic solvents on the stability of free and immobilized *MpCAR* is shown in Figure 5. This study is intended to explore the potential of *MpCAR* for industrial applications, as organic solvents are commonly used to increase substrate solubility and suppress water-dependent side reactions [44]. The free and immobilized *MpCAR* showed stability in 25% (*v/v*) of most hydrophilic, polar solvents ($\log p \leq 1$), as proven by their relative catalytic activities, which retained >50% (Figure 5). In contrast, when treated with organic solvents with $\log p \geq 1$ (non-polar or hydrophobic organic solvents), the free *MpCAR* showed a deleterious effect in their catalytic activities compared to the control. It was possibly due to the presence of organic solvents, which caused conformational changes that may have led to enzyme deactivation. Moreover, hydrophobic organic solvents have a dramatic effect on enzyme properties. At lower water content, the enzymes became too dry; thus, they lost their flexibility, resulting in inefficient catalysis [45]. Water acting as a lubricant promotes conformational mobility required for optimal catalysis. It was in concurrence with previous studies whereby the flexibility of lipase B from *Candida antarctica* was reduced when treated with high $\log p$ values of organic solvents [46]. The flexibility of subtilisin from *Bacillus licheniformis* was also found to be lower in octane ($\log p = 4.183$) as compared to in acetonitrile ($\log p = -0.334$) [47]. Nevertheless, in this study, there were still *MpCAR* activities observed (~20–60% relative activities) when it was treated with hydrophobic solvents such as chloroform, octanol, and xylene. Most likely, the support Seplite LX120 was able to protect *MpCAR* from environmental changes when exposed to the solvents.

The free *MpCAR* was found to possess higher relative activity after being exposed to hydrophilic and polar organic solvents as compared to the immobilized *MpCAR*. This phenomenon is probably due to the conformation of the enzyme during its free form, which seems to enhance the enzyme's ability to catalyze higher substrate conversion in the presence of organic solvents. Even though the immobilized enzyme has lower relative activity when treated with 25% (*v/v*) of hydrophilic solvents, the effect was not significantly detrimental. The support used in this study may not help maintain the enhanced relative activity of *MpCAR* when treated with organic solvents, as obtained by the free *MpCAR*. However, compared to the control, the hydrophilic solvents did not inhibit the activity of the immobilized enzyme, as more than 100% of the relative activity of

MpCAR was still observed in dimethyl sulfoxide (DMSO), methanol, ethanol, 1-propanol, and butanol. This immobilization strategy could stabilize *MpCAR* towards organic solvents by preventing the enzyme from unfolding and malfunctioning at its active site caused by solvent penetration [48].

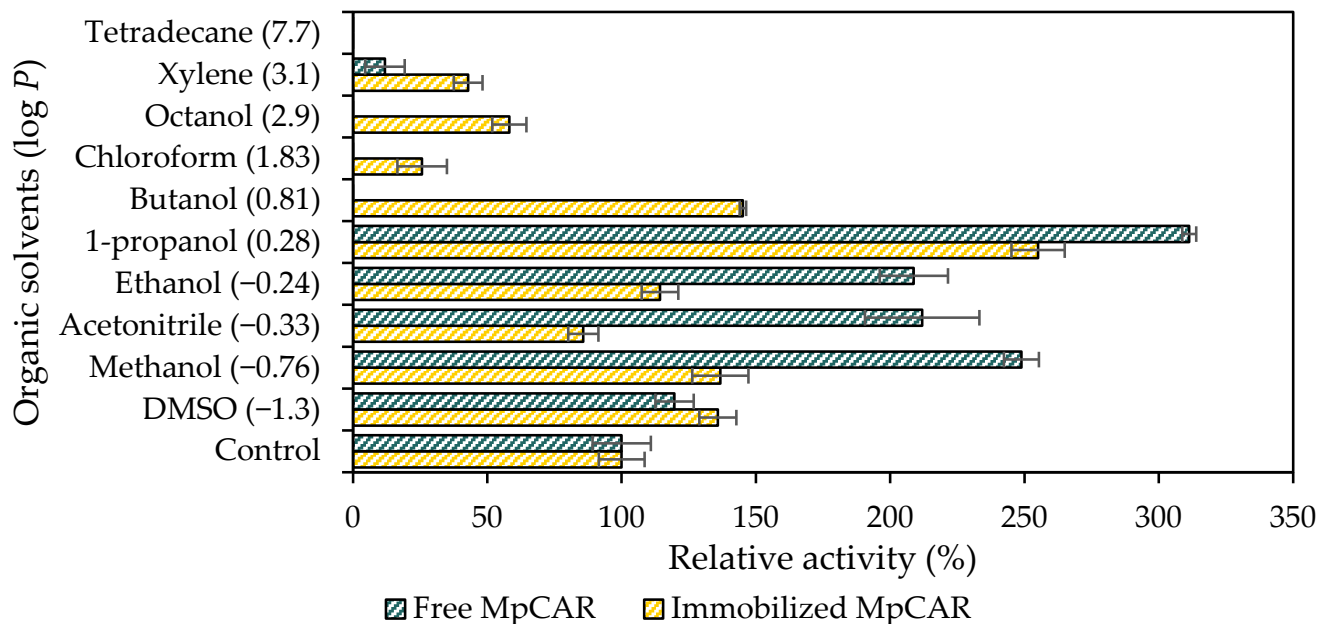


Figure 5. Effect of organic solvents on the stability of free and immobilized carboxylic acid reductase from *Mycobacterium phlei* (*MpCAR*). Green columns: relative activity of free *MpCAR*; yellow columns: relative activity of immobilized *MpCAR* onto Seplite LX120. $\log p$ is the partition coefficient of the solvent between water and octanol. Samples were measured in triplicates.

3.5. Morphology Analysis Using SEM

SEM micrographs (Figure 6A–D) revealed the morphology of the empty Seplite LX120 support to have a non-porous structure at 20 \times , 500 \times , 5000 \times , and 10,000 \times magnifications. For comparison, the morphology of immobilized *MpCAR* was also observed at the same magnifications (Figure 6E–H). At 20 \times magnification, it was observed that Seplite LX120 is a non-porous spherical in shape support (Figure 6A,B). After immobilizing *MpCAR* on the support, the void and crack areas became less obvious and most likely to be filled up and covered by the adsorbed *MpCAR* (Figure 6G,H). As seen in Figure 6G,H, the support with adsorbed enzyme shows a compact and continuous structure after the enzyme immobilization, as compared with the structure of an empty support at 5000 \times and 10,000 \times magnifications. Similar SEM images were observed when UDP-glucosyltransferase and sucrose synthase were co-immobilized onto a heterofunctional resin [49]. The decrease in surface roughness and visibility of the spatial position of the support, as shown by SEM images, verified the successful enzyme immobilization [50].

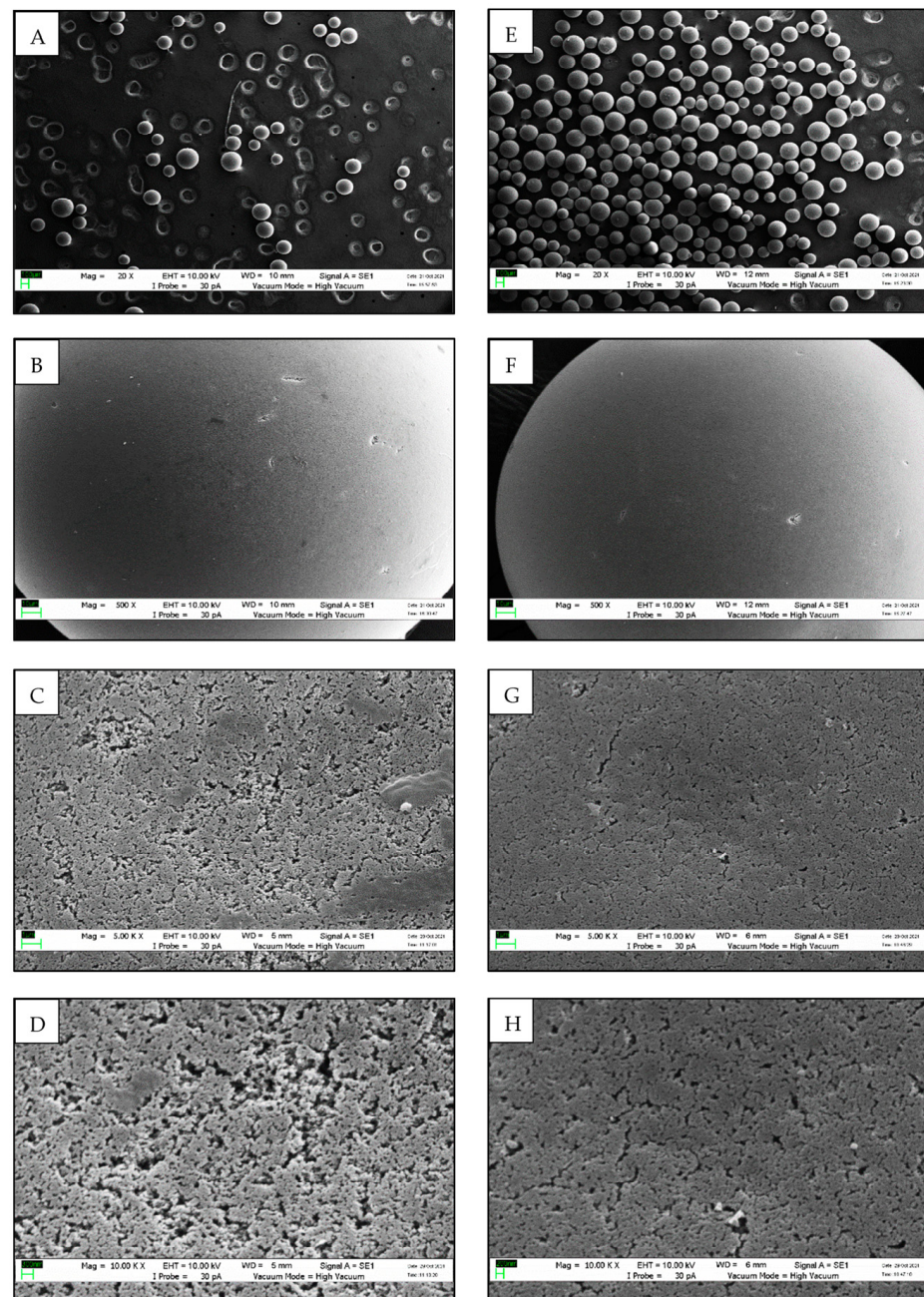


Figure 6. Scanning Electron Microscopy (SEM) images of empty Seplite LX120 and immobilized carboxylic acid reductase from *Mycobacterium phlei* (*MpCAR*) at 20 \times , 500 \times , 5000 \times , and 10,000 \times magnifications. Images (A–D) refer to empty Seplite LX120. Images (E–H) refer to immobilized *MpCAR* on Seplite LX120.

3.6. Surface Area Analysis Using BET

BET analysis revealed that the surface area decreased from 122.3347 m²/g before *MpCAR* immobilization to 108.5485 m²/g after immobilization. There was also a slight decrease in the adsorption and desorption pore diameter of the support after the immobilization process (from 0.734 to 0.733 nm and from 7.286 to 7.226 nm of adsorption and desorption pore diameter, respectively). Reduction of the pore volume of Seplite LX120 support was also observed after immobilization (from 0.022 to 0.020 cm³/g and from 0.223 to 0.196 cm³/g of adsorption and desorption pore volume, respectively). The reduction in surface area, pore diameter, and pore volume indicated that the *MpCAR* enzyme was successfully adsorbed onto the support. Similar BET analysis results were obtained when

lipase and laccase were immobilized onto chicken eggshells and Fe₂O₃ yolk-shell particles, respectively [18,51]. It is proven that upon immobilization, *MpCAR* filled up some of the spaces of the pores on the immobilization support, resulting in a decrease in surface area, pore diameter, and pore volume.

Figure 7A,B show the N₂ adsorption-desorption isotherm test results to further describe the support capacity or affinity towards *MpCAR*. Based on IUPAC recommendations, the adsorption isotherms before and after immobilization were categorized as Type II isotherms, and were commonly obtained when the adsorption took place on nonporous or macroporous materials (Figure 7A,B) [52]. By comparing Figure 7A,B, the quantity of nitrogen adsorbed slightly decreased after *MpCAR* immobilization, implying that there were fewer pores available after immobilization as most of the pores were occupied by the carboxylic acid reductase [53].

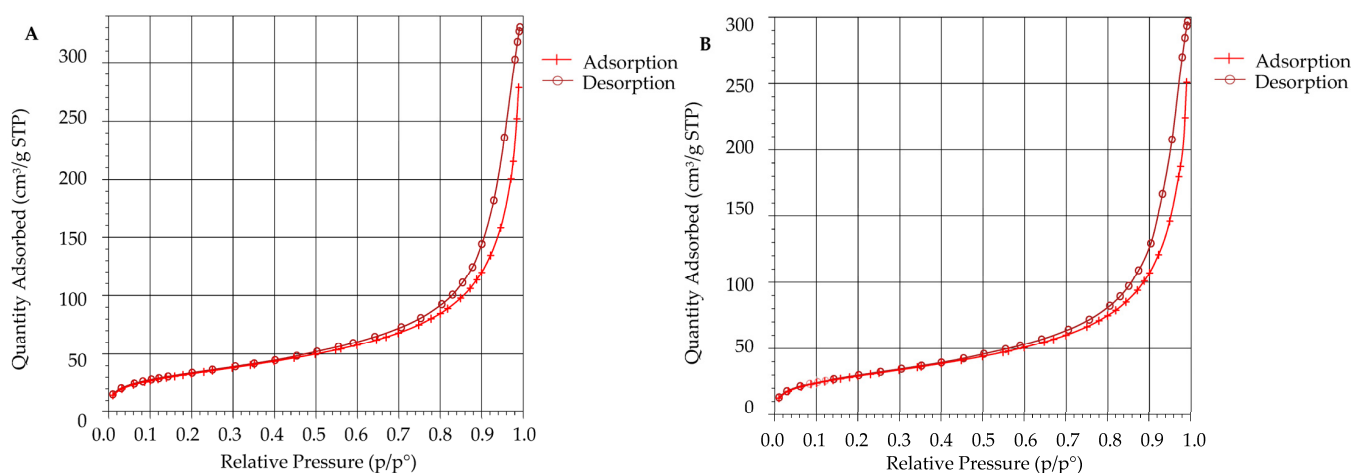


Figure 7. Nitrogen adsorption-desorption isotherm plots of Seplite LX120, before (A) and after (B) immobilization of carboxylic acid reductase from *Mycobacterium phlei* (*MpCAR*).

3.7. Structural Analysis Using FTIR

FTIR spectroscopy analysis was used to investigate the bonds involved in the attachment of *MpCAR* onto the support. Figure 8 shows the overlaid FTIR profiles for all samples, which exhibited similar peak spectra with slight differences. The overlapped OH and NH groups' strong vibrations of empty Seplite LX120 and free *MpCAR* can be seen at wavenumbers ranging from 3200 to 3400 cm⁻¹. The peak of free *MpCAR* may be more obvious compared to the peak of immobilized *MpCAR* at this same wavenumber range, most likely due to the presence of water molecules when the enzyme is in its free form (in liquid form) as compared to when the *MpCAR* was immobilized onto the support and dried [54]. Since this FTIR spectroscopy analysis was conducted without the standard calibration curve of known concentrations, the results obtained in this section remain qualitative [55]. The peaks of amine stretch detected in this region were sufficient to confirm the presence of the enzyme and the amine functional group of the support in all samples. The bands correlated with protein conformations were detected in the range of 1500–1800 cm⁻¹ wavenumbers for all samples, including the empty support since the support is composed of an amine functional group. The changes and shift of peaks (Figure 8) within this range of wavenumbers, including N-H bending vibrations (Amide II at 1550 cm⁻¹) and C=O stretching (Amide I at 1650 cm⁻¹), indicate that there were alterations in protein secondary structures [50]. These changes indicated that the adsorption of *MpCAR* onto Seplite LX120 successfully occurred, as similarly discovered when Amano lipase A was immobilized onto a silica matrix [51]. FTIR was also used to examine the changes in the secondary structures of lipase from *Rhizimucor miehei* immobilized onto chitosan as part of the characterization study [56]. In addition, amide bands detected here clearly indicated the preserved enzyme activity after immobilization [57].

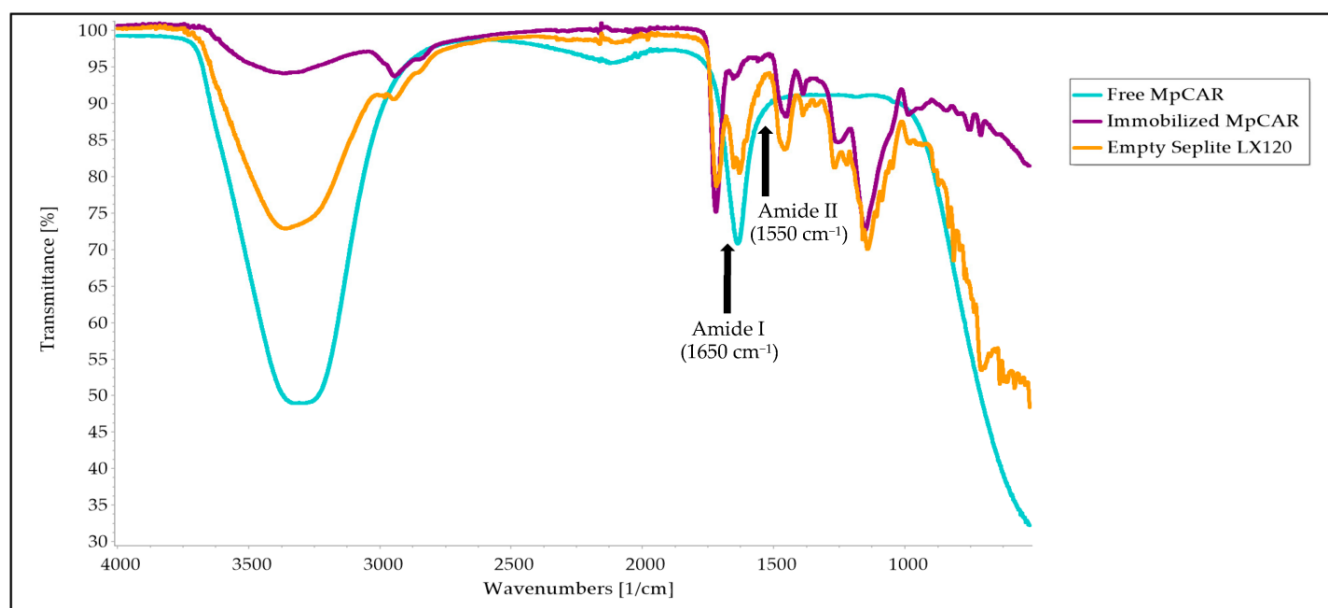


Figure 8. Overlaid Fourier-Transform Infrared Spectroscopy (FTIR) profiles of free carboxylic acid reductase from *Mycobacterium phlei* (*MpCAR*), immobilized *MpCAR* onto Seplite LX120, and empty Seplite LX120. Blue line: Free *MpCAR*; Purple line: Immobilized *MpCAR*; Orange line: Empty Seplite LX120.

3.8. Storage Stability and Reusability

The stability of the biocatalyst was performed by conducting a series of activity assays for two months of storage for immobilized *MpCAR*, while for free *MpCAR*, it was conducted for one month. Storage stability is important for long-term usage, especially in large-scale applications [58]. The long-term storage of immobilized enzymes may contribute to better practicality and cost-effectiveness of the enzymatic process. Upon the immobilization process, the interaction between the support and the enzyme is more robust, which, in this case, may improve the attachment of the carboxylic acid reductase molecule, thus resulting in better storage stability. The storage stability of the immobilized *MpCAR* was better than the free *MpCAR* at 4 °C and 25 °C (room temperature) (Figure 9A,B). The immobilized *MpCAR* retained 45.13% of its initial activity after 8 weeks at 4 °C and 27.41% after 8 weeks at 25 °C. The relative activity of free *MpCAR* drastically dropped to 29% after 4 weeks at 4 °C and 16.33% after 4 weeks of storage at 25 °C. The decrease in free *MpCAR* enzyme activity could be attributed to enzyme denaturation caused by the conditions and storage period [59]. As for the immobilized *MpCAR*, the aggregation or unfolding process of the enzyme would be less likely to occur as the enzymes were well attached to the support. Other immobilized oxidoreductases also showed better storage stability than their free form after being immobilized [60].

The reusability of the immobilized *MpCAR* is presented in Figure 9C. The reusability assay can be considered as one of the parameters that would be beneficial for industrial applications. Increased reusability can lower production costs by reducing the amount of free CAR in industrial production. Though immobilization conditions have been optimized, enzyme leaching or inactivation may impede the operational stability and repeated use of the immobilized enzyme [61]. In this study, the immobilized *MpCAR* was repeatedly assayed for several cycles to measure its reusability. It was observed that the immobilized *MpCAR* retained 59.68% of its catalytic activity even after 10 times of usage. Likewise, immobilization of CAR from *Pycnoporus cinnabarinus* (*PcCAR2*) showed good reusability as it retained >80% of its initial activity after six cycles of activity assay [30]. Based on the Bradford assay conducted in this study, *MpCAR* was not detected in the supernatant of the reaction mixture even after 10 cycles of the assay (data not shown). This shows that enzyme leaching was not one of the factors for residual activity reduction of immobilized *MpCAR*.

after being reused repeatedly. The presence of an amine ($-NH_2$) functional group in the polymer backbone (support) could facilitate strong interactions via hydrophilic-hydrophilic interaction or ionic bonding with the enzyme [62]. The decline in residual activity toward consecutive cycles might be associated with the partial inactivation of the enzyme [63]. Nevertheless, the high reusability of immobilized *MpCAR* still provides a strong reason for its application in industries.

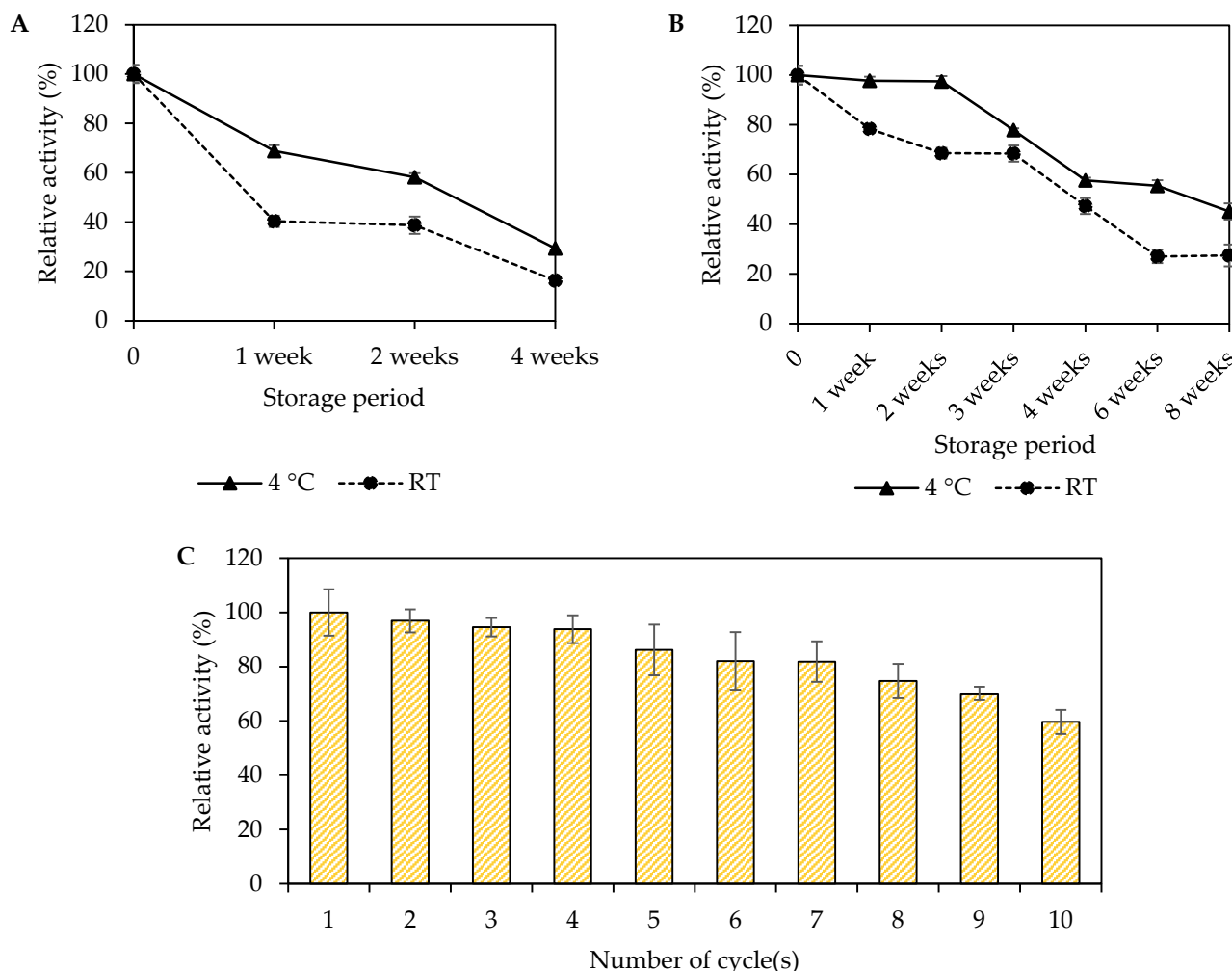


Figure 9. (A,B) Storage stabilities of free and immobilized *Mycobacterium phlei* carboxylic acid reductase (*MpCAR*) on Seplite LX120 with optimized immobilization conditions, and (C) reusability of immobilized *MpCAR*. Both free (A) and immobilized (B) *MpCAR* were stored for a period of time at 4 and 25 °C (room temperature). The relative activity (%) at day 0 of storage was referred to as 100%. For (C), the initial activity of the immobilized *MpCAR* was taken as 100%. Samples were measured in triplicates.

3.9. Bioconversion Using Immobilized *MpCAR*

Besides the biochemical and biophysical properties of the immobilized enzyme, the ability of the immobilized enzyme to convert substrate to the desired product is also an important parameter that needs to be assessed. Hence, in this study, the preliminary experiment on the bioconversion of benzoic acid to benzaldehyde using immobilized *MpCAR* was evaluated at different incubation temperatures ranging from 20 to 60 °C, and the benzaldehyde product was quantified using HPLC-UV. These temperatures were chosen since this *MpCAR* was previously known as a moderately thermostable enzyme [26]. Plus, benzoic acid was selected as the substrate since it is a standard substrate for most carboxylic acid reductases. Based on Figure 10, the bioconversion yield, and the benzaldehyde

concentration increased gradually from 20 to 60 °C. The temperature increment causes the molecular movement rate to increase; hence, the reaction rate also increases [64]. The immobilized *MpCAR* achieved the highest conversion of benzoic acid at 60 °C. The bioconversion yield of 52% at 60 °C, equivalent to 2.6 mM of benzaldehyde, indicated that immobilized *MpCAR* preferred a higher temperature for its catalytic activity. Almost no benzaldehyde was detected at lower temperatures, such as at 20 °C. A previous study revealed that ~50% of bioconversion of 5 mM of benzoic acid was achieved by immobilized CAR from *Segniliparus rugosus* (*SrCAR*) after 18 h of incubation at 30 °C [29]. Another finding showed that ~80% bioconversion yield was achieved by immobilized *PcCAR*, given 2 mM of benzoic acid was supplied for 1 h of reaction incubation at 25 °C [30]. Here, the 2.6 mM of benzaldehyde was quantified after 1 h of incubation of immobilized *MpCAR* at 60 °C, even though the yield was only about 50%. These findings agree with the trend of optimal activity based on the NADPH consumption assay of immobilized *MpCAR*, as discussed in Section 3.2 (Figure 3A). Conclusively, at a moderately higher temperature, a greater amount of substrate can be converted to a product with an active immobilized *MpCAR*. This study demonstrated that the adsorption of *MpCAR* onto the polymeric support Seplite LX120 was a good approach for maintaining the thermostability of the enzyme. This preliminary bioconversion study of immobilized *MpCAR* should be a starting point for further exploration of a better bioconversion by the immobilized enzyme, which may include various other carboxylic acid substrates.

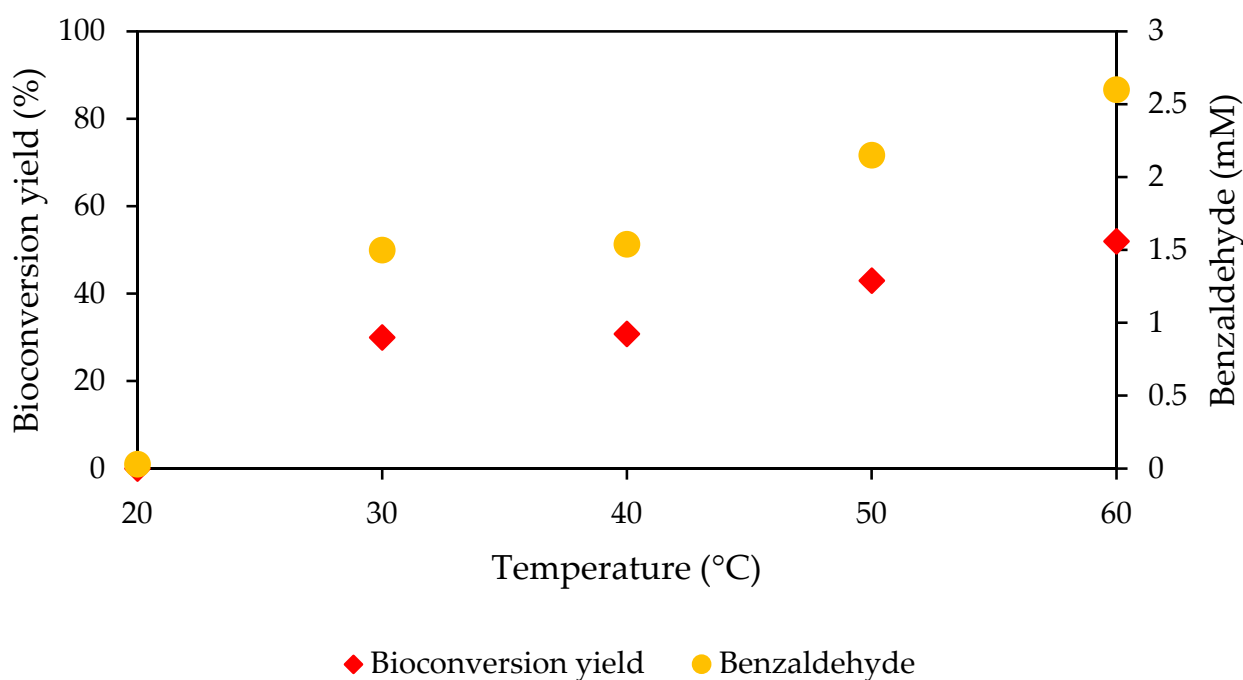


Figure 10. Bioconversion of immobilized carboxylic acid reductase from *Mycobacterium phlei* (*MpCAR*) onto Seplite LX120. The immobilized *MpCAR* was incubated with other assay components for 1 h at temperatures ranging from 20 to 60 °C prior to product analysis using HPLC-UV. The substrate concentration supplied was 5 mM. The bioconversion yield (%) and benzaldehyde (mM) concentration were calculated.

4. Conclusions

For the first time, the immobilization of *MpCAR* onto a commercial support, Seplite LX120, was successfully conducted via adsorption. The immobilized *MpCAR* showed improved biochemical properties, as the enzyme retained its activity over broad temperature and pH ranges. Both free and immobilized *MpCAR* were stable when treated with 25% (*v/v*) polar organic solvents. The immobilized enzyme was found to be able to be stored longer at 4 and 25 °C compared to the free enzyme. Via immobilization of *MpCAR*

onto Seplite LX120, the operational stability of the enzyme may reach up to 10 cycles. The morphological characterization using SEM showed that the enzyme was successfully adsorbed onto the Seplite LX120 as the cracks and void areas on the support were covered after the immobilization process, as seen in the 10,000 \times magnification images. Based on the structural characterization using FTIR analysis, there were changes in the secondary structures of the protein after being immobilized onto Seplite LX120 as detected between 1500–1800 cm^{-1} wavenumbers. Nevertheless, the FTIR analysis also confirmed that the activity of the MpCAR was still preserved after immobilization. The BET analysis supported that the immobilization of MpCAR by adsorption technique was successful since the surface area, pore volume, and pore diameter of Seplite LX120 decreased after the immobilization process. Interestingly, HPLC-UV analysis proved that the immobilized MpCAR was active and could convert benzoic acid to benzaldehyde at a higher temperature, at least up to 60 °C of incubation temperature. Overall, the MpCAR immobilized onto Seplite LX120 could be one of the promising biocatalysts for aldehyde production in the flavor and fragrance industries, dependent on its significant improvement in properties, as discussed above.

Author Contributions: Conceptualization, M.S.M.A. and R.S.B.; methodology, M.S.M.A. and R.S.B.; validation, R.N.Z.R.A.R., M.S.M.A., N.H.A.K. and W.L.; formal analysis, R.S.B.; investigation, R.S.B.; resources, M.S.M.A., R.N.Z.R.A.R., N.H.A.K. and W.L.; data curation, M.S.M.A. and R.S.B.; writing—original draft preparation, R.S.B.; writing—review and editing, R.N.Z.R.A.R., M.S.M.A., N.H.A.K. and W.L.; supervision, R.N.Z.R.A.R., M.S.M.A. and N.H.A.K.; funding acquisition, R.N.Z.R.A.R., M.S.M.A. and N.H.A.K. All authors have read and agreed to the published version of the manuscript.

Funding: The authors would like to thank PETRONAS Research Sdn. Bhd. (PRSB) for funding this project (UPMCS 2019-75/1021) and the Graduate Research Fellowship (GRF) from Universiti Putra Malaysia (UPM) for financial assistance and sponsorship.

Institutional Review Board Statement: Not applicable.

Data Availability Statement: Not applicable.

Conflicts of Interest: The authors declare no conflict of interest.

References

1. Napora-Wijata, K.; Strohmeier, G.A.; Winkler, M. Biocatalytic reduction of carboxylic acids. *Biotechnol. J.* **2014**, *9*, 822–843. [[CrossRef](#)]
2. Li, T.; Rosazza, J.P.N. Purification, characterization, and properties of an aryl aldehyde oxidoreductase from *Nocardia* sp. strain NRRL 5646. *J. Bacteriol.* **1997**, *179*, 3482–3487. [[CrossRef](#)]
3. Kunjapur, A.M.; Prather, K.L.J. Microbial engineering for aldehyde synthesis. *Appl. Environ. Microbiol.* **2015**, *81*, 1892–1901. [[CrossRef](#)]
4. Kato, N.; Joung, E.H.; Yang, H.C.; Masuda, M.; Shimao, M.; Yanase, H. Purification and characterization of aromatic acid reductase from *Nocardia asteroides* JCM 3016. *Agric. Biol. Chem.* **1991**, *55*, 757–762. [[CrossRef](#)]
5. Gahlloth, D.; Aleku, G.A.; Leys, D. Carboxylic acid reductase: Structure and mechanism. *J. Biotechnol.* **2020**, *307*, 107–113. [[CrossRef](#)]
6. He, A.; Li, T.; Daniels, L.; Fotheringham, I.; Rosazza, J.P.N. *Nocardia* sp. carboxylic acid reductase: Cloning, expression, and characterization of a new aldehyde oxidoreductase family. *Appl. Environ. Microbiol.* **2004**, *70*, 1874–1881. [[CrossRef](#)]
7. Venkatasubramanian, P.; Daniels, L.; Rosazza, J.P.N. Reduction of carboxylic acids by *Nocardia* aldehyde oxidoreductase requires a phosphopantetheinylated enzyme. *J. Biol. Chem.* **2007**, *282*, 478–485. [[CrossRef](#)]
8. Qu, G.; Guo, J.; Yang, D.; Sun, Z. Biocatalysis of carboxylic acid reductases: Phylogenesis, catalytic mechanism and potential applications. *Green Chem.* **2018**, *20*, 777–792. [[CrossRef](#)]
9. Atsumi, S.; Wu, T.-Y.; Eckl, E.-M.; Hawkins, S.D.; Buelter, T.; Liao, J.C. Engineering the isobutanol biosynthetic pathway in *Escherichia coli* by comparison of three aldehyde reductase/alcohol dehydrogenase genes. *Appl. Microbiol. Biotechnol.* **2010**, *85*, 651–657. [[CrossRef](#)] [[PubMed](#)]
10. Kramer, L.; Hankore, E.D.; Liu, Y.; Liu, K.; Jimenez, E.; Guo, J.; Niu, W. Characterization of carboxylic acid reductases for biocatalytic synthesis of industrial chemicals. *ChemBioChem* **2018**, *19*, 1452–1460. [[CrossRef](#)] [[PubMed](#)]
11. Sheppard, M.J.; Kunjapur, A.M.; Wenck, S.J.; Prather, K.L.J. Retro-biosynthetic screening of a modular pathway design achieves selective route for microbial synthesis of 4-methyl-pentanol. *Nat. Commun.* **2014**, *5*, 5031. [[CrossRef](#)] [[PubMed](#)]

12. Napora-Wijata, K.; Robins, K.; Osorio-Lozada, A.; Winkler, M. Whole-cell carboxylate reduction for the synthesis of 3-hydroxytyrosol. *ChemCatChem* **2014**, *6*, 1089–1095. [[CrossRef](#)]
13. Venkitasubramanian, P.; Daniels, L.; Das, S.; Lamm, A.S.; Rosazza, J.P.N. Aldehyde oxidoreductase as a biocatalyst: Reductions of vanillic acid. *Enzyme Microb. Technol.* **2008**, *42*, 130–137. [[CrossRef](#)] [[PubMed](#)]
14. Datta, S.; Christena, L.R.; Rajaram, Y.R.S. Enzyme immobilization: An overview on techniques and support materials. *3 Biotech.* **2013**, *3*, 1–9. [[CrossRef](#)] [[PubMed](#)]
15. Zdarta, J.; Meyer, A.S.; Jesionowski, T.; Pinelo, M. Developments in support materials for immobilization of oxidoreductases: A comprehensive review. *Adv. Colloid Interface Sci.* **2018**, *258*, 1–20. [[CrossRef](#)] [[PubMed](#)]
16. Zhu, C.Y.; Li, F.L.; Zhang, Y.W.; Gupta, R.K.; Patel, S.K.S.; Lee, J.K. Recent strategies for the immobilization of therapeutic enzymes. *Polymers* **2022**, *14*, 1409. [[CrossRef](#)] [[PubMed](#)]
17. Patel, S.K.S.; Choi, H.; Lee, J.K. Multimetal-based inorganic-protein hybrid system for enzyme immobilization. *ACS Sustain. Chem. Eng.* **2019**, *7*, 13633–13638. [[CrossRef](#)]
18. Patel, S.K.S.; Anwar, M.Z.; Kumar, A.; Otari, S.V.; Pagolu, R.T.; Kim, S.Y.; Kim, I.W.; Lee, J.K. Fe₂O₃ yolk-shell particle-based laccase biosensor for efficient detection of 2,6-dimethoxyphenol. *Biochem. Eng. J.* **2018**, *132*, 1–8. [[CrossRef](#)]
19. Lyu, X.; Gonzalez, R.; Horton, A.; Li, T. Immobilization of enzymes by polymeric materials. *Catalysts* **2021**, *11*, 1211. [[CrossRef](#)]
20. Jia, Y.; Chen, Y.; Luo, J.; Hu, Y. Immobilization of laccase onto meso-MIL-53 (Al) via physical adsorption for the catalytic conversion of triclosan. *Ecotoxicol. Environ. Saf.* **2019**, *184*, 109670. [[CrossRef](#)] [[PubMed](#)]
21. Liu, D.M.; Chen, J.; Shi, Y.P. Tyrosinase immobilization on aminated magnetic nanoparticles by physical adsorption combined with covalent crosslinking with improved catalytic activity, reusability and storage stability. *Anal. Chim. Acta* **2018**, *1006*, 90–98. [[CrossRef](#)] [[PubMed](#)]
22. Ahmed, S.A.; Mostafa, F.A.; Ouis, M.A. Enhancement stability and catalytic activity of immobilized α -amylase using bioactive phospho-silicate glass as a novel inorganic support. *Int. J. Biol. Macromol.* **2018**, *112*, 371–382. [[CrossRef](#)] [[PubMed](#)]
23. Shao, B.; Liu, Z.; Zeng, G.; Liu, Y.; Yang, X.; Zhou, C.; Chen, M.; Liu, Y.; Jiang, Y.; Yan, M. Immobilization of laccase on hollow mesoporous carbon nanospheres: Noteworthy immobilization, excellent stability and efficacious for antibiotic contaminants removal. *J. Hazard. Mater.* **2019**, *362*, 318–326. [[CrossRef](#)] [[PubMed](#)]
24. Kuribayashi, L.M.; Ribeiro, V.P.D.R.; de Santana, R.C.; Ribeiro, E.J.; dos Santos, M.G.; Falleiros, L.N.S.S.; Guidini, C.Z. Immobilization of β -galactosidase from *Bacillus licheniformis* for application in the dairy industry. *Appl. Microbiol. Biotechnol.* **2021**, *105*, 3601–3610. [[CrossRef](#)]
25. Guidini, C.Z.; Fischer, J.; Santana, L.N.S.; Cardoso, V.L.; Ribeiro, E.J. Immobilization of *Aspergillus oryzae* β -galactosidase in ion exchange resins by combined ionic-binding method and cross-linking. *Biochem. Eng. J.* **2010**, *52*, 137–143. [[CrossRef](#)]
26. Finnigan, W.; Thomas, A.; Cromar, H.; Gough, B.; Snajdrova, R.; Adams, J.P.; Littlechild, J.A.; Harmer, N.J. Characterization of carboxylic acid reductases as enzymes in the toolbox for synthetic chemistry. *ChemCatChem* **2017**, *9*, 1005–1017. [[CrossRef](#)]
27. Thomas, A.; Cutlan, R.; Finnigan, W.; van der Mark, G.; Harmer, N. Highly thermostable carboxylic acid reductases generated by ancestral sequence reconstruction. *Commun. Biol.* **2019**, *2*, 429. [[CrossRef](#)]
28. Finnigan, W.; Cutlan, R.; Snajdrova, R.; Adams, J.P.; Littlechild, J.A.; Harmer, N.J. Engineering a seven enzyme biotransformation using mathematical modelling and characterized enzyme parts. *ChemCatChem* **2019**, *11*, 3474–3489. [[CrossRef](#)]
29. Thompson, M.P.; Derrington, S.R.; Heath, R.S.; Porter, J.L.; Mangas-Sanchez, J.; Devine, P.N.; Truppo, M.D.; Turner, N.J. A generic platform for the immobilisation of engineered biocatalysts. *Tetrahedron* **2019**, *75*, 327–334. [[CrossRef](#)]
30. Maphatsoe, M.M.; Hashem, C.; Ling, J.G.; Horvat, M.; Rumbold, K.; Bakar, F.D.A.; Winkler, M. Characterization and immobilization of *Pycnoporus cinnabarinus* carboxylic acid reductase, PcCAR2. *J. Biotechnol.* **2022**, *345*, 47–54. [[CrossRef](#)]
31. Bradford, M.M. A rapid and sensitive method for the quantitation of microgram quantities of protein utilizing the principle of protein-dye binding. *Anal. Biochem.* **1976**, *254*, 248–254. [[CrossRef](#)]
32. Akhtara, M.K.; Turner, N.J.; Jones, P.R. Carboxylic acid reductase is a versatile enzyme for the conversion of fatty acids into fuels and chemical commodities. *Proc. Natl. Acad. Sci. USA* **2013**, *110*, 87–92. [[CrossRef](#)] [[PubMed](#)]
33. Horvat, M.; Winkler, M. In vivo reduction of medium- to long-chain fatty acids by carboxylic acid reductase (CAR) enzymes: Limitations and solutions. *ChemCatChem* **2020**, *12*, 5076–5090. [[CrossRef](#)]
34. Costa, V.M.; de Souza, M.C.M.; Fehine, P.B.A.; Macedo, A.C.; Gonçalves, L.R.B. Nanobiocatalytic systems based on lipase-Fe₃O₄ and conventional systems for isoniazid synthesis: A comparative study. *Braz. J. Chem. Eng.* **2016**, *33*, 661–673. [[CrossRef](#)]
35. Liu, G.; Sun, L.; Wu, X.; Zhang, W.; Feng, J.; Cui, Y.; Lu, Z.; Shen, J.; Liu, Z.; Yuan, S. Immobilization of puerarin glycosidase from *Microbacterium oxydans* CGMCC 1788 increases puerarin transformation efficiency. *Braz. J. Chem. Eng.* **2014**, *31*, 325–333. [[CrossRef](#)]
36. Keerti; Gupta, A.; Kumar, V.; Dubey, A.; Verma, A.K. Kinetic characterization and effect of immobilized thermostable β -glucosidase in alginate gel beads on sugarcane juice. *ISRN Biochem.* **2014**, *2014*, 178498. [[CrossRef](#)]
37. Wu, E.; Li, Y.; Huang, Q.; Yang, Z.; Wei, A.; Hu, Q. Laccase immobilization on amino-functionalized magnetic metal organic framework for phenolic compound removal. *Chemosphere* **2019**, *233*, 327–335. [[CrossRef](#)]
38. Bayramoğlu, G.; Yalçın, E.; Arica, M.Y. Immobilization of urease via adsorption onto L-histidine-Ni(II) complexed poly(HEMA-MAH) microspheres: Preparation and characterization. *Process Biochem.* **2005**, *40*, 3505–3513. [[CrossRef](#)]
39. Erginer, R.; Toppare, L.; Alkan, S.; Bakir, U. Immobilization of invertase in functionalized copolymer matrices. *React. Funct. Polym.* **2000**, *45*, 227–233. [[CrossRef](#)]

40. Hung, T.C.; Giridhar, R.; Chiou, S.H.; Wu, W.T. Binary immobilization of *Candida rugosa* lipase on chitosan. *J. Mol. Catal. B Enzym.* **2003**, *26*, 69–78. [[CrossRef](#)]
41. Miao, Q.; Zhang, C.; Zhou, S.; Meng, L.; Huang, L.; Ni, Y.; Chen, L. Immobilization and characterization of pectinase onto the cationic polystyrene resin. *ACS Omega* **2021**, *6*, 31683–31688. [[CrossRef](#)]
42. Cao, M.; Li, Z.; Wang, J.; Ge, W.; Yue, T.; Li, R.; Colvin, V.L.; Yu, W.W. Food related applications of magnetic iron oxide nanoparticles: Enzyme immobilization, protein purification, and food analysis. *Trends Food Sci. Technol.* **2012**, *27*, 47–56. [[CrossRef](#)]
43. Almulaiky, Y.Q.; Al-Harbi, S.A. A novel peroxidase from Arabian balsam (*Commiphora gileadensis*) stems: Its purification, characterization and immobilization on a carboxymethylcellulose/Fe₃O₄ magnetic hybrid material. *Int. J. Biol. Macromol.* **2019**, *133*, 767–774. [[CrossRef](#)] [[PubMed](#)]
44. Kumar, A.; Dhar, K.; Kanwar, S.S.; Arora, P.K. Lipase catalysis in organic solvents: Advantages and applications. *Biol. Proced. Online* **2016**, *18*, 2. [[CrossRef](#)]
45. Wang, S.; Meng, X.; Zhou, H.; Liu, Y.; Secundo, F.; Liu, Y. Enzyme stability and activity in non-aqueous reaction systems: A mini review. *Catalysts* **2016**, *6*, 32. [[CrossRef](#)]
46. Trodler, P.; Pleiss, J. Modeling structure and flexibility of *Candida antarctica* lipase B in organic solvents. *BMC Struct. Biol.* **2008**, *8*, 9. [[CrossRef](#)] [[PubMed](#)]
47. Fasoli, E.; Ferrer, A.; Barletta, G.L. Hydrogen/deuterium exchange study of subtilisin carlsberg during prolonged exposure to organic solvents. *Biotechnol. Bioeng.* **2009**, *102*, 1025–1032. [[CrossRef](#)] [[PubMed](#)]
48. Stepankova, V.; Bidmanova, S.; Koudelakova, T.; Prokop, Z.; Chaloupkova, R.; Damborsky, J. Strategies for stabilization of enzymes in organic solvents. *ACS Catal.* **2013**, *3*, 2823–2836. [[CrossRef](#)]
49. Chu, J.; Yue, J.; Qin, S.; Li, Y.; Wu, B.; He, B. Biocatalysis for rare ginsenoside Rh₂ production in high level with co-immobilized UDP-glycosyltransferase *Bs-YjiC* mutant and sucrose synthase *AtSuSy*. *Catalysts* **2021**, *11*, 132. [[CrossRef](#)]
50. Liao, L.; Meng, Y.; Wang, R.; Jia, B.; Li, P. Coupling and regulation of porous carriers using plasma and amination to improve the catalytic performance of glucose oxidase and catalase. *Front. Bioeng. Biotechnol.* **2019**, *7*, 426. [[CrossRef](#)]
51. Shahrin, N.A.; Yong, G.G.; Serri, N.A. Fructose stearate esterify in packed bed reactor using immobilized lipase. *IOP Conf. Ser. Mater. Sci. Eng.* **2020**, *716*, 012017. [[CrossRef](#)]
52. Sarma, G.K.; Gupta, S.S.; Bhattacharyya, K.G. Removal of hazardous basic dyes from aqueous solution by adsorption onto kaolinite and acid-treated kaolinite: Kinetics, isotherm and mechanistic study. *SN Appl. Sci.* **2019**, *1*, 211. [[CrossRef](#)]
53. Adnan, M.; Li, K.; Xu, L.; Yan, Y. X-shaped ZIF-8 for immobilization *Rhizomucor miehei* lipase via encapsulation and its application toward biodiesel production. *Catalysts* **2018**, *8*, 96. [[CrossRef](#)]
54. Seki, T.; Chiang, K.Y.; Yu, C.C.; Yu, X.; Okuno, M.; Hunger, J.; Nagata, Y.; Bonn, M. The bending mode of water: A powerful probe for hydrogen bond structure of aqueous systems. *J. Phys. Chem. Lett.* **2020**, *11*, 8459–8469. [[CrossRef](#)]
55. Kowalczyk, D.; Pitucha, M. Application of FTIR method for the assessment of immobilization of active substances in the matrix of biomedical materials. *Materials* **2019**, *12*, 2972. [[CrossRef](#)] [[PubMed](#)]
56. Collins, S.E.; Lassalle, V.; Ferreira, M.L. FTIR-ATR characterization of free *Rhizomucor miehei* lipase (RML), Lipozyme RM im and chitosan-immobilized RML. *J. Mol. Catal. B Enzym.* **2011**, *72*, 220–228. [[CrossRef](#)]
57. Delfino, I.; Portaccio, M.; Della Ventura, B.; Mita, D.G.; Lepore, M. Enzyme distribution and secondary structure of sol-gel immobilized glucose oxidase by micro-attenuated total reflection FT-IR spectroscopy. *Mater. Sci. Eng. C* **2013**, *33*, 304–310. [[CrossRef](#)]
58. Basso, A.; Serban, S. Industrial applications of immobilized enzymes—A review. *Mol. Catal.* **2019**, *479*, 110607. [[CrossRef](#)]
59. Iyer, P.V.; Ananthanarayan, L. Enzyme stability and stabilization—Aqueous and non-aqueous environment. *Process Biochem.* **2008**, *43*, 1019–1032. [[CrossRef](#)]
60. Guzik, U.; Hupert-Kocurek, K.; Wojcieszynska, D. Immobilization as a strategy for improving enzyme properties—Application to oxidoreductases. *Molecules* **2014**, *19*, 8995–9018. [[CrossRef](#)] [[PubMed](#)]
61. Anwar, M.Z.; Kim, D.J.; Kumar, A.; Patel, S.K.S.; Otari, S.; Mardina, P.; Jeong, J.-H.; Sohn, J.-H.; Kim, J.H.; Park, J.T.; et al. SnO₂ hollow nanotubes: A novel and efficient support matrix for enzyme immobilization. *Sci. Rep.* **2017**, *7*, 1533. [[CrossRef](#)]
62. Handayani, N.; Loos, K.; Wahyuningrum, D.; Buchari; Zulfikar, M.A. Immobilization of *Mucor miehei* lipase onto macroporous aminated polyethersulfone membrane for enzymatic reactions. *Membranes* **2012**, *2*, 198–213. [[CrossRef](#)]
63. Patel, S.K.S.; Gupta, R.K.; Kim, S.Y.; Kim, I.W.; Kalia, V.C.; Lee, J.K. *Rhus vernicifera* laccase immobilization on magnetic nanoparticles to improve stability and its potential application in bisphenol A degradation. *Indian J. Microbiol.* **2021**, *61*, 45–54. [[CrossRef](#)]
64. Robinson, P.K. Enzymes: Principles and biotechnological applications. *Essays Biochem.* **2015**, *59*, 1–41. [[CrossRef](#)]